A NOVEL SUPPRESSION STRATEGY OF DC SIDE POWER FLUCTUATION IN CONVERTER WITH VSG CONTROL

Wangwang Bai,* Dezhou Yang,* Zhongdan Zhang,* Wanwei Li,* and Ping Cai*

Abstract

A DC side power fluctuation exists in the converter with virtual synchronous generator (VSG) control under the unbalanced grid voltage. It will affect the service life of battery equipment. This paper proposes a direct-feedforward-voltage control method to suppress the DC side power fluctuation in the inverter under the unbalanced grid voltage. Firstly, based on the equivalent circuit of the inverter in the rotating coordinate frame, the reason causing the DC side power fluctuation is obtained. The variables affecting the fluctuation are achieved. Secondly, a direct-feedforward-voltage control method to eliminate the fluctuation is proposed, in which the modulation wave is modified to generate an additional voltage in the inverter output voltage. Through interacting with the positive sequence current and the unbalanced grid voltage, a feedforward voltage is generated to eliminate the fluctuation of the DC side power. The feedforward voltage is formed by the negative sequence voltage of the power grid, the positive sequence output current, and the positive sequence output voltage. Finally, the control characteristics of the proposed control method are presented. Based on analysis of the power closed-loop transfer function, the proposed control method has a small influence on the power closed-loop and can achieve the power control precision of the VSG. Simulation and experimental results are proposed to verify the analysis and the effectiveness of the proposed control method of suppressing the DC side power fluctuation.

Key Words

Virtual synchronous generator (VSG), unbalanced grid voltage, power fluctuation, inverter

1. Introduction

With the development of renewable energy and distributed power generators, the high proportion of renewable energy connected to the grid will influence on the power system [1]–[3]. In renewable energy generation, such as wind power and photovoltaic power, due to the influence of meteorological factors, these new energy sources have characteristics, such as intermittency, randomness, and volatility, resulting in fluctuations in output power [4]. In addition, the widespread use of power electronic devices will gradually increase the proportion of power sources with asynchronous generator characteristics. The inertia of asynchronous generator power sources is relatively small because the inertia size reflects the frequency anti-interference ability of the power system, that is, the frequency stability. The increasing proportion of asynchronous power sources with smaller inertia may lead to frequency stability issues. Therefore, in existing methods, controlling renewable energy generation as a virtual synchronous generator (VSG) is an effective solution [5], [6].

About the study on VSG, many papers have conducted detailed research. As a result, under the unbalanced grid voltages, there is a power fluctuation problem on the DC side of VSG. Previous literature has conducted in-depth research on the VSG control. For example, in [7], power sharing among multiple VSGs is studied. Multiple VSGs can operate stably and share active and reactive power. Under the condition of unbalanced grid voltages, the VSG control will be affected [8]–[10], and the power fluctuation at twice the fundamental frequency will occur [11], [12]. In situations requiring minimal DC side power fluctuation, the active power on the AC side of the inverter must remain constant, and the DC side power or voltage should be kept constant. For example, when the DC side contains a battery, in order to reduce the fluctuation of battery charging and discharging power, the DC side power of the inverter needs to be constant.

There are many methods to suppress power fluctuations on the DC side. The analysis and summary on this point can be expressed. And, the method in previous literature has a slight drawback. In the traditional method mentioned in the previous literature, in order to suppress fluctuating power, the inverter with the VSG control generates a negative sequence current, which eliminates the power fluctuation caused by the unbalanced grid voltage. The method of controlling the positive and negative

* Economic and Technological Research Institute of State Grid Gansu Electric Power Company, Lanzhou, China; 1241509352@qq.com; yangdzh@vip.sina.com; {13109365848, liwanw82, 18361221379}@163.com
Corresponding author: Wangwang Bai

Recommended by Amirthagunaraj Yogarathnam
(DOI: 10.2316/J.2025.203-0577)

sequence components separately is actually to obtain the unbalanced current generated by the inverter with the VSG control. The unbalanced current will interact with the unbalanced grid voltage to obtain a constant power. At present, there are two types of suppressing methods existing in the literature. The one is to suppress the power fluctuation through the DC side voltage control loop. For example, in [13] and [14], the DC side voltage control is used to suppress the fluctuation. But, the methods are not suitable for the VSG control, because the dynamic response of the active power in the VSG is slower than that of the methods in the literature. The other method of suppressing the power fluctuation is to control the positive and negative sequence currents of the grid-connected inverter separately. For example, in [15]–[19], the reference values of the positive and the negative sequence currents in grid-connected inverters are obtained, and current closed-loops are applied to control the positive and negative sequence currents separately. As a result, the power can be controlled to a constant value. In [20] and [21], in order to suppress the power fluctuation, a method of adding a negative sequence current is proposed. This method suppresses the power fluctuation by adding a negative sequence current closed-loop, which is connected in parallel with the positive sequence current closed-loop. The above methods can suppress the steady-state power fluctuation. However, when the positive sequence current closed-loop and the negative sequence current closed-loop operate in parallel, if there is a difference in the parameters of the two current closed-loops, the current closed-loops will affect each other in the dynamic process, which will reduce the effectiveness of the power fluctuation suppression.

This paper aims to address the shortcomings of control methods in existing literature and proposes a more optimal control method. This paper realises a novel suppression strategy of the power fluctuation based on the direct-feedforward-voltage control in the inverter with a VSG control. On the basis of the original VSG control, this paper introduces a voltage feedforward control that directly modifies the modulation wave of the PWM control, enabling the inverter to output the added voltage. The added voltage will interact with the unbalanced grid voltage and the positive sequence current to eliminate the power fluctuation at twice the fundamental frequency, ultimately achieving a constant DC side power. The contributions of this paper can be summarised as follows: a novel control strategy of suppressing the power fluctuation is presented; this control strategy does not affect the current control in the dynamic process.

2. DC Side Power Under Unbalanced Grid Voltage

2.1 Control of VSG

The control of VSG includes the active power–frequency control and the reactive power–voltage control. Firstly, in the control system, the model of VSG is proposed. Then, the control diagram can be obtained by using the model of VSG. The equation for the output voltage of the synchronous generator is shown in (1), and its rotor

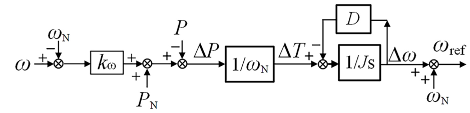

Figure 1. Control diagram of active power–frequency control of VSG.

motion equation is shown in (2) [22]–[25]. Among them, u_a, u_b, and u_c represent the output voltages, u_{Ia}, u_{Ib}, and u_{Ic} represent the induction electromotive force of stator winding, i_a, i_b, and i_c represent the output currents, J is the moment of inertia of the synchronous generator (kg·m^2), T_m is the mechanical torque of the generator (N·m), T_e is the electromagnetic torque of the synchronous generator (N·m), ω is the rotation speed of the synchronous generator (rad/s), D is the damping coefficient, ω_N is the rated value of the rotation speed of the synchronous generator (rad/s), P_N is the rated value of the active power (W), P is the output active power (W), k_ω is the coefficient of the relationship between active power and frequency, U_N is the rated value of the output voltage (V), U is the output voltage (V), Q_N is the rated value of the reactive power (var), Q is the output reactive power (var), k_u is the coefficient of the relationship between the reactive power and the voltage. In the equations, $D\Delta\omega$ reflects the damping effect when the rotation speed changes. The VSG control utilises an inverter to simulate the active power–frequency droop output characteristics and the reactive power–voltage droop output characteristics of a synchronous generator, while considering the stator voltage equation and the rotor motion equation of the synchronous generator, so that the energy storage inverter can simulate the external characteristics of the synchronous machine. By substituting the expression of the droop characteristic of the synchronous generator into the expression of the rotor motion equation of the synchronous generator, the (3) can be obtained. The active power–frequency control block diagram of the VSG control can be obtained in Fig. 1. In the control block diagram, the virtual mechanical power P_N is obtained through the droop characteristic of the active power–frequency of the synchronous generator, and the change in torque is obtained by the output electromagnetic power. Finally, the reference value of the rotation speed is obtained through the damping coefficient and the moment of inertia in the rotor motion equation [26]–[28]. The excitation control system of the synchronous generator has been simplified to obtain a virtual excitation controller, and its control diagram is shown in Fig. 2. In the control diagram, the actual measured reactive power is subtracted from its rated value, and the resulting difference is then multiplied by a corresponding coefficient to determine the voltage difference due to the change in reactive power. Then the voltage reference value of the VSG voltage control loop is obtained by adding the voltage difference to the rated voltage of the power grid. After the feedback voltage is subtracted from this reference, a virtual excitation current is produced by a PI regulator. Due to the linear relationship between the excitation current and the amplitude of the induced electromotive force of the VSG, the control of the

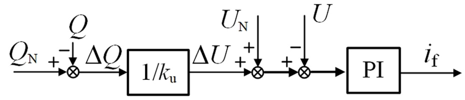

Figure 2. Control diagram of reactive power–voltage control of VSG.

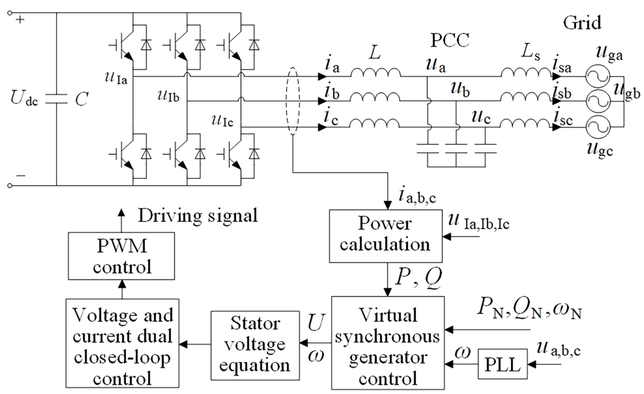

Figure 3. Block diagram of inverter with VSG control.

induced electromotive force of the VSG can be achieved by adjusting the excitation current.

$$\begin{bmatrix} u_a \\ u_b \\ u_c \end{bmatrix} = \begin{bmatrix} u_{\mathrm{Ia}} \\ u_{\mathrm{Ib}} \\ u_{\mathrm{Ic}} \end{bmatrix} - L\frac{d}{dt}\begin{bmatrix} i_a \\ i_b \\ i_c \end{bmatrix} \tag{1}$$

$$J\frac{d\omega}{dt} = T_m - T_e - D \cdot \Delta\omega \tag{2}$$

$$\begin{aligned} J\frac{d\omega}{dt} &= T_m - T_e - D \cdot \Delta\omega \\ &= \frac{(\omega_N - \omega)\, k_\omega + P_N - P}{\omega} - D \cdot \Delta\omega. \end{aligned} \tag{3}$$

The inverter with VSG control is formed by the main circuit and the control system. The three-phase inverter with LCL filter is used, and the grid voltages will affect the VSG. The control system includes the VSG control and the voltage-current-dual-loop control. In the inverter, the VSG control is shown in Fig. 3. The power system is equivalent to a voltage source with an impedance. The inverter is controlled as a VSG, and the DC side power is provided by renewable energy generation or batteries. u_a, u_b, and u_c represent the PCC voltages, u_{Ia}, u_{Ib}, and u_{Ic} represent the AC output voltages of the inverter, and i_a, i_b, and i_c represent the output currents of the inverter. i_{sa}, i_{sb}, and i_{sc} represent the grid currents. u_{ga}, u_{gb}, and u_{gc} represent the grid voltages.

2.2 Analysis of DC Side Power Fluctuation

The analysis of the DC side power fluctuation is proposed. With the relationship between the voltage and the current, the power is obtained. Then, the second harmonic power fluctuation on the DC side can be derived. The model of the main circuit is shown in (4). When the three-phase voltage of the power grid is unbalanced, the power grid voltage includes positive and negative sequence components. In a three-phase three wire system, there is no zero sequence component. In the rotating coordinate frame, the positive and negative sequence components are separated. The (5) can be obtained, where the superscript "p" represents the positive sequence component and the superscript "n" represents the negative sequence component. u_{Id}^p, u_{Iq}^p, u_{Id}^n, and u_{Iq}^p are respectively the negative and positive components of the inverter output voltages, i_d^n, i_q^n, i_d^p, and i_q^p are respectively the negative and positive components of the inverter output currents. u_d^n, u_q^n, u_d^p, and u_q^p are respectively the negative and positive components of the PCC voltages. The active power and reactive power are shown in (6) where the variables are shown in (7). In (6), when the grid voltage is unbalanced, the output active power and reactive power of the inverter with the VSG control are composed of DC components (p_0 and q_0) and second order harmonic components ($p_1\cos2\omega t$, $p_2\cos2\omega t$, $q_1\sin2\omega t$, and $q_2\sin2\omega t$), respectively. The power flowing from the AC side to the DC side of the inverter is shown in (8). According to (8), the second order harmonic component in the output power of the inverter will cause a second harmonic fluctuation in the DC bus voltage. If the DC side is a battery, it may cause the battery to repeatedly charge and discharge, reducing its service life. Therefore, it is necessary to suppress the second harmonic power fluctuation.

$$\begin{cases} u_{\mathrm{Ia}} = L\frac{di_a}{dt} + u_a \\ u_{\mathrm{Ib}} = L\frac{di_b}{dt} + u_b \\ u_{\mathrm{Ic}} = L\frac{di_c}{dt} + u_c \end{cases} \tag{4}$$

$$\begin{cases} u_{\mathrm{Id}}^p = L\frac{di_d^p}{dt} - \omega L i_q^p + u_d^p \\ u_{\mathrm{Iq}}^p = L\frac{di_q^p}{dt} + \omega L i_d^p + u_q^p \\ u_{\mathrm{Id}}^n = L\frac{di_d^n}{dt} + \omega L i_q^n + u_d^n \\ u_{\mathrm{Iq}}^n = L\frac{di_q^n}{dt} - \omega L i_q^n + u_q^n \end{cases} \tag{5}$$

$$\begin{cases} p\,(t) = p_0 + p_1\cos 2\omega t + p_2 \sin 2\omega \mathrm{t} \\ q\,(t) = q_0 + q_1 \cos 2\omega t + q_2 \sin 2\omega t \end{cases} \tag{6}$$

$$\begin{cases} p_0 = 1.5\left(u_{\mathrm{Id}}^p i_d^p + u_{\mathrm{Iq}}^p i_q^p + u_{\mathrm{Id}}^n i_d^n + u_{\mathrm{Iq}}^n i_q^n\right) \\ p_1 = 1.5\left(u_{\mathrm{Id}}^p i_d^n + u_{\mathrm{Iq}}^p i_q^n + u_{\mathrm{Id}}^n i_d^p + u_{\mathrm{Iq}}^n i_q^p\right) \\ p_2 = 1.5\left(u_{\mathrm{Iq}}^n i_d^p - u_{\mathrm{Id}}^n i_q^p - u_{\mathrm{Iq}}^p i_d^n + u_{\mathrm{Id}}^p i_q^n\right) \\ q_0 = 1.5\left(u_{\mathrm{Iq}}^p i_d^p - u_{\mathrm{Id}}^p i_q^p + u_{\mathrm{Iq}}^n i_d^n - u_{\mathrm{Id}}^n i_q^n\right) \\ q_1 = 1.5\left(u_{\mathrm{Iq}}^p i_d^n - u_{\mathrm{Id}}^p i_q^n + u_{\mathrm{Iq}}^n i_d^p - u_{\mathrm{Id}}^n i_q^p\right) \\ q_2 = 1.5\left(u_{\mathrm{Id}}^p i_d^n + u_{\mathrm{Iq}}^p i_q^n - u_{\mathrm{Id}}^n i_d^p - u_{\mathrm{Iq}}^n i_q^p\right) \end{cases} \tag{7}$$

$$\frac{1}{2}\frac{d(CU_{\mathrm{dc}}^2)}{dt} = p(t). \tag{8}$$

2.3 Proposed Strategy for Suppressing DC Side Power Fluctuations Under Unbalanced Grid Voltage

Based on the relationship equations between the voltage and the current under unbalanced grid voltage, the power

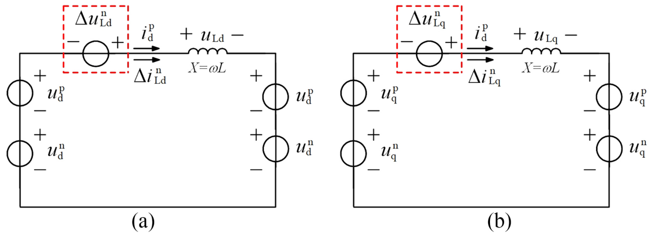

Figure 4. Equivalent circuit of power fluctuation suppression strategy when three-phase voltages are unbalanced: (a) Equivalent circuit in d-axis and (b) Equivalent circuit in q-axis.

fluctuation suppression strategy is proposed from the equivalent circuits. The power fluctuation suppression strategy in this paper is to add a feedforward voltage on the modulation wave, which generates an output voltage to suppress the power fluctuation. The principle is as follows: by changing the modulation wave, the negative sequence voltages Δu_{Ld}^n and Δu_{Lq}^n are added to the output voltage, which interacts with the positive sequence voltage and the positive sequence current, generates a new second order harmonic power. The sum of this second order harmonic power fluctuation and the previous second order harmonic power fluctuation is zero, then the second harmonic order power fluctuation is eliminated. The analysis of the power fluctuation can be presented in Fig. 4. Substituting Δu_{Ld}^n and Δu_{Lq}^n into the second order harmonic power fluctuation expression in (6) and making the second order harmonic power fluctuation expression 0, (9) can be obtained. Based on the relationship between voltage and current in the equivalent circuit, (10) can be obtained. Solving (10) can obtain the values of $\Delta u_{\mathrm{Ld}}^n$and Δu_{Lq}^nwhich are shown in (11). If the inverter outputs the added values $\Delta u_{\mathrm{Ld}}^n$and Δu_{Lq}^n, the second order harmonic power fluctuation can be suppressed. In Fig. 4, $u_d^p + u_d^n$ and $u_q^p + u_q^n$ are the output voltages of the proposed control strategy. Δi_{Ld}^n and Δi_{Lq}^n are the changed currents after Δu_{Ld}^n and Δu_{Lq}^n are added.

$$
\begin{cases}
u_d^n i_d^p + u_q^n i_q^p + \Delta u_{\mathrm{Ld}}^n i_d^p + \Delta u_{\mathrm{Lq}}^n i_q^p + u_d^p \Delta i_{\mathrm{Ld}}^n + u_q^p \Delta i_{\mathrm{Lq}}^n = 0 \\
-u_d^n i_q^p + u_q^n i_d^p - \Delta u_{\mathrm{Ld}}^n i_q^p + \Delta u_{\mathrm{Lq}}^n i_d^p - u_d^p \Delta i_{\mathrm{Lq}}^n + u_q^p \Delta i_{\mathrm{Ld}}^n = 0
\end{cases} \tag{9}
$$

$$
\begin{cases}
u_d^n i_d^p + u_q^n i_q^p + \Delta u_{\mathrm{Ld}}^n i_d^p + \Delta u_{\mathrm{Lq}}^n i_q^p + u_d^p \frac{\Delta u_{\mathrm{Ld}}^n}{\omega \mathrm{L}} + u_q^p \frac{\Delta u_{\mathrm{Lq}}^n}{\omega \mathrm{L}} = 0 \\
-u_d^n i_q^p + u_q^n i_d^p - \Delta u_{\mathrm{Ld}}^n i_q^p + \Delta u_{\mathrm{Lq}}^n i_d^p - u_d^p \frac{\Delta u_{\mathrm{Lq}}^n}{\omega \mathrm{L}} + u_q^p \frac{\Delta u_{\mathrm{Ld}}^n}{\omega \mathrm{L}} = 0
\end{cases} \tag{10}
$$

The proposed strategy for suppressing the power fluctuation under unbalanced grid voltage is proposed. The feedforward voltage for suppressing the power fluctuation is generated. And, the control diagram can also be obtained. The feedforward voltage can be calculated from (11). The strategy for suppressing the DC side voltage fluctuation under unbalanced grid voltage is shown in Fig. 5. The dashed line represents the fluctuation suppression part, and the modulation wave is modified through adding a negative sequence voltage Δu_{Ld}^n and Δu_{Lq}^n to the output voltage, ultimately eliminating the power fluctuation of the DC side. In Fig. 5, the voltage reference is generated by (12), where $C_{abc/dq}$ are the rotation transformation matrix from the abc coordinate to the dq coordinate [28].

$$
\begin{cases}
\Delta u_{\mathrm{Ld}}^n = \dfrac{\left(-u_d^n i_q^p + u_q^n i_d^p\right)\left(i_q^p + \frac{u_q^p}{\omega \mathrm{L}}\right) - \left(u_d^n i_d^p + u_q^n i_q^p\right)\left(i_d^p - \frac{u_d^p}{\omega \mathrm{L}}\right)}{\left[\left(i_d^p + \frac{u_d^p}{\omega \mathrm{L}}\right)\left(i_d^p - \frac{u_d^p}{\omega \mathrm{L}}\right) - \left(\frac{u_q^p}{\omega L - i_q^p}\right)\left(i_q^p + \frac{u_q^p}{\omega \mathrm{L}}\right)\right]} \\
\Delta u_{\mathrm{Lq}}^n = \dfrac{\left(-u_d^n i_q^p + u_q^n i_d^p\right)\left(i_d^p + \frac{u_d^p}{\omega \mathrm{L}}\right) - \left(u_d^n i_d^p + u_q^n i_q^p\right)\left(\frac{u_q^p}{\omega L - i_q^p}\right)}{\left[\left(i_q^p + \frac{u_q^p}{\omega \mathrm{L}}\right)\left(\frac{u_q^p}{\omega L - i_q^p}\right) - \left(i_d^p - \frac{u_d^p}{\omega \mathrm{L}}\right)\left(i_d^p + \frac{u_d^p}{\omega \mathrm{L}}\right)\right]}
\end{cases} \tag{11}
$$

$$
\begin{bmatrix} u_{\mathrm{dref}} \\ u_{\mathrm{qref}} \end{bmatrix} = C_{abc/dq} \begin{bmatrix} U_{\mathrm{ref}} \sin\left(\omega_{\mathrm{ref}} t\right) \\ U_{\mathrm{ref}} \sin\left(\omega_{\mathrm{ref}} t - \frac{2\pi}{3}\right) \\ U_{\mathrm{ref}} \sin\left(\omega_{\mathrm{ref}} t + \frac{2\pi}{3}\right) \end{bmatrix}. \tag{12}
$$

This paper compares the proposed method with the traditional method. The dynamic response in the proposed method and the traditional method is different. And the convergence performance in the proposed method and the traditional method is also different. The traditional suppression strategy is shown in [15]–[19]. The negative current control loop is added to the control system in the literature. For the power fluctuation suppression, the traditional strategy is a closed-loop control, while the

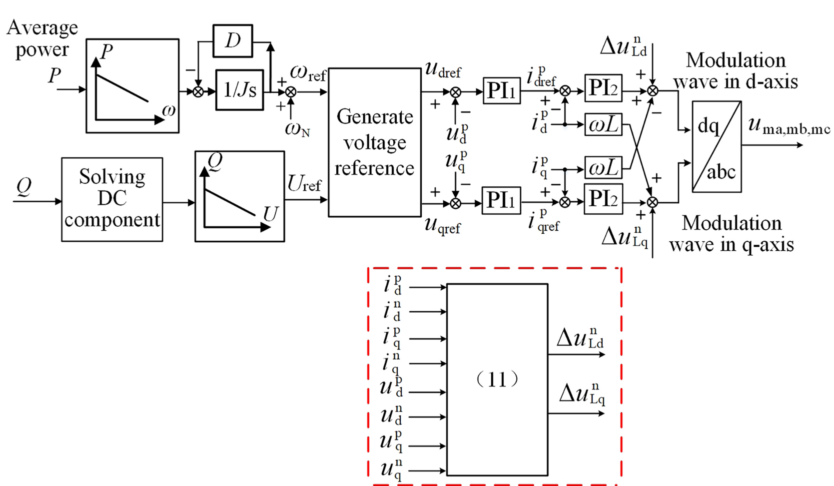

Figure 5. The proposed strategy for suppressing the power fluctuation under unbalanced grid voltage.

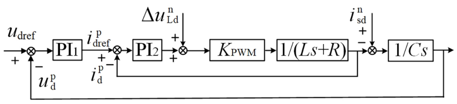

Figure 6. Diagram of voltage control closed-loop.

proposed strategy employs open-loop control. In term of the dynamic response, the proposed suppression strategy has a faster dynamic response than that of the traditional suppression strategy. That is, when the DC side power changes, the proposed strategy responds quickly and has a better suppression effect on the power fluctuation. Regarding the convergence under disturbance, due to its open-loop control, the proposed strategy has weaker convergence performance compared to the traditional strategy.

2.4 Control Characteristics of the Active Power Under Unbalanced Grid Voltage

The control characteristics of the active power under unbalanced grid voltage are analysed in this part. Firstly, the transfer functions are proposed. Then, the control characteristics are obtained through the Bode plots and the control diagrams. As shown in Fig. 5, the voltage and current dual closed-loop control is applied. The voltage closed-loop control diagram of the inverter with the VSG control is shown in Fig. 6. After subtracting the reference voltage from the output voltage of the inverter, the reference current is generated through the PI_1 regulator. Then, through current closed-loop control, the output current tracks the reference current. The d-axis and q-axis include the voltage and current dual closed-loops, respectively. This paper takes the d-axis voltage and current dual closed-loop control as an example for analysis. In Fig. 6, the SPWM of the inverter is represented by a proportion component shown as K_{PWM}. R is the internal resistance of the inverter inductor. The capacitor current is obtained by subtracting the inverter's output current from the power supply current, and the inverter voltage is then calculated by multiplying this current by 1/Cs. Both closed-loops are negative feedback control loops, and after reaching steady state, the output voltage of the inverter is equal to the reference voltage. An additional Δu^n_{Ld} is added to the modulation wave, and its transfer function is shown in (13). The Bode plot of the closed-loop transfer function under a set of parameters is shown in Fig. 7. The parameters are: $K_{p1} = 0.01$, $K_{p2} = 40$, $K_{PWM} = 1$, $L = 2$ mH, $C = 10\ \mu$F, $R = 0.01\ \Omega$. It can be seen that adding Δu^n_{Ld} to the modulation wave can make the output voltage include this voltage value. The power control block diagram of the inverter with the VSG control is shown in Fig. 8. Among them, U_g represents the positive sequence voltage of the power grid, U represents the output voltage of the inverter, the line impedance is X, the phase angle difference between the inverter output voltage and the grid voltage is φ, ω_N is the rated speed, E^* represents the amplitude of the reference grid voltage. When the voltage in the power grid is unbalanced, there is a power fluctuation at twice the fundamental frequency, which is represented by Δp, and $\Delta p = p_1\cos 2\omega t + p_2\sin 2\omega t$. $G_{v1}(s)$ is the closed-loop transfer function (fromu^p_d to u_{dref}) of the voltage control loop, and $G_{v2}(s)$ is the closed-loop transfer function (fromu^p_d to Δu^n_{Ld}). $G_{v1}(s)$ reflects the precision of the voltage control loop, and $G_{v2}(s)$ reflects the influence of the disturbance of the voltage control loop. K_{p1} and K_{p2} are respectively the proportional regulator coefficient. K_{PWM} is the proportional coefficient of the PWM control.

$$\begin{cases} G_{V1}(s) = \frac{u^p_d}{u_{\text{dref}}} = \frac{K_{p1}K_{p2}K_{\text{PWM}}}{\text{Cs}(Ls+R+K_{p2}K_{\text{PWM}})+K_{p1}K_{p2}K_{\text{PWM}}} \\ G_{V2}(s) = \frac{u^p_d}{\Delta u^n_{\text{Ld}}} = \frac{K_{\text{PWM}}}{K_{p2}K_{\text{PWM}}(Cs-K_{p1})+Cs(Ls+R)} \end{cases}. \tag{13}$$

The transfer function of the active power control closed-loop is obtained in this part. The influence of the second order harmonic power fluctuation is analysed. Then, the control characteristics are obtained through the Bode plots. The transfer function of the active power control closed-loop in the inverter with the VSG control is expressed in (14). The natural frequency and damping are

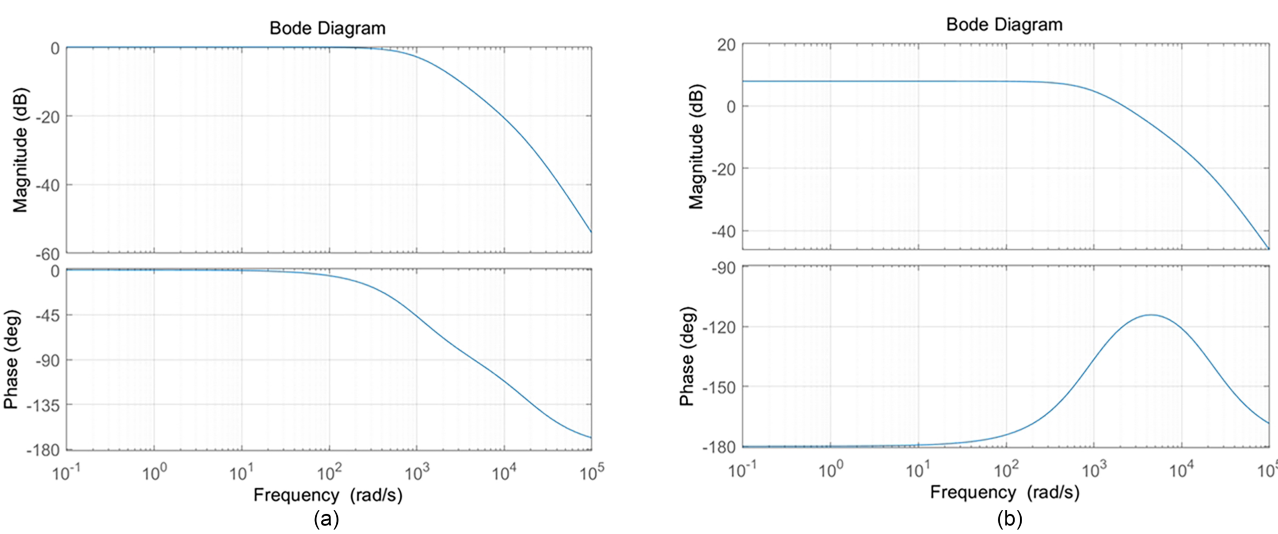

Figure 7. Bode diagram of voltage control closed-loop: (a) Bode plot of GV1(s) and (b) Bode plot of GV2(s).

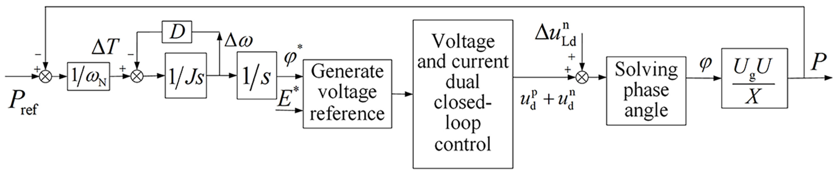

Figure 8. The power control block diagram of the inverter with the VSG control.

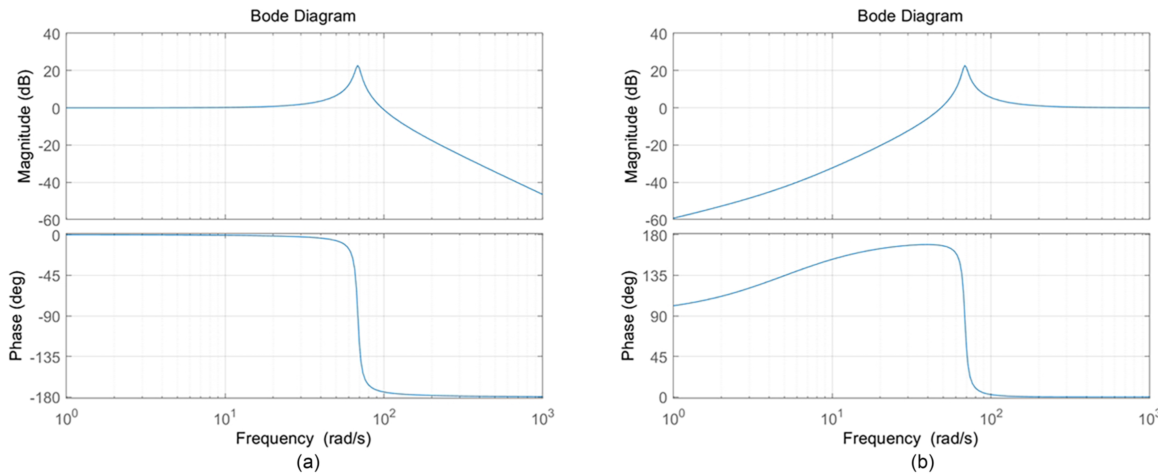

Figure 9. Bode diagram of active power control closed-loop: (a) Bode plot of $G_1(s)$ and (b) Bode plot of $G_2(s)$.

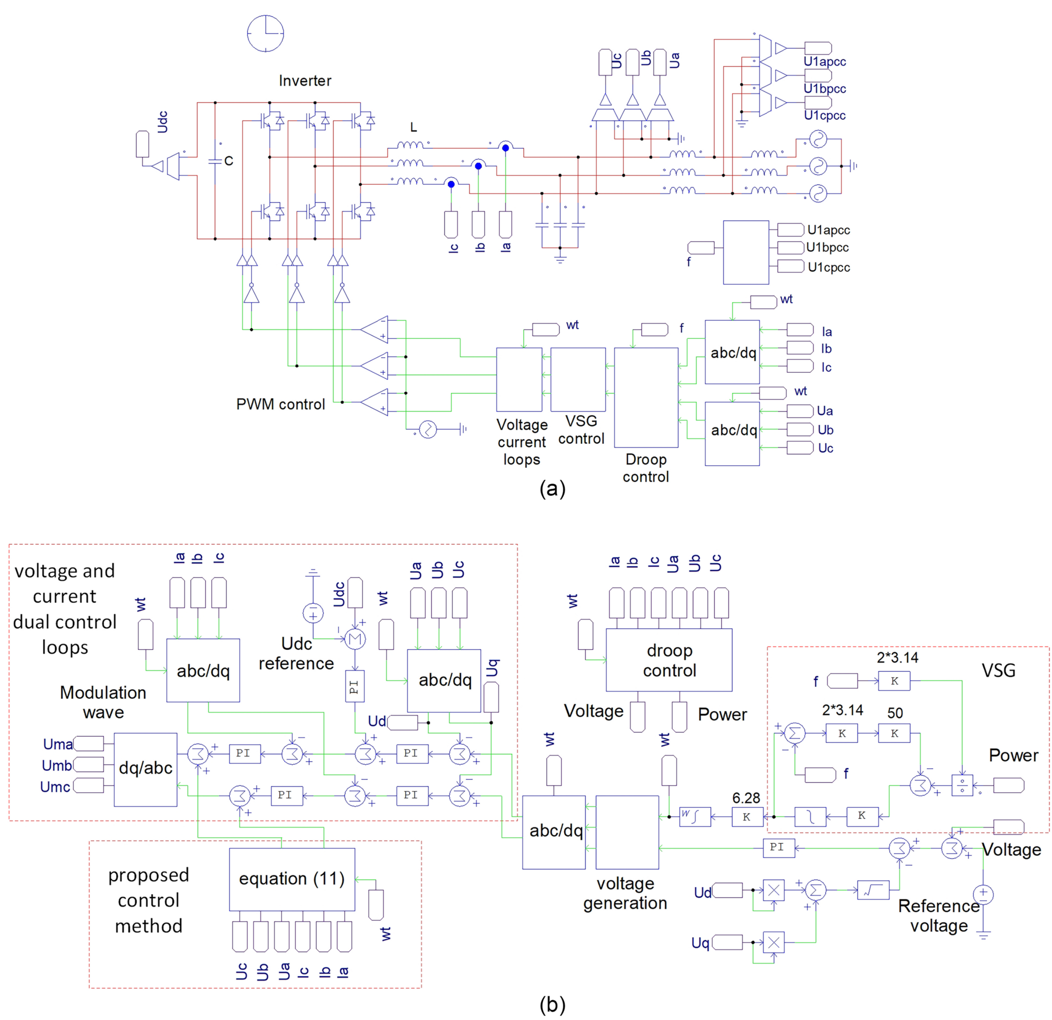

Figure 10. Simulation model of proposed suppression strategy: (a) block diagram of simulation system and (b) control system.

shown in (15). The closed-loop transfer function between the fluctuating power and the output power is shown in (16). The Bode plot under a set of parameters can be obtained from (14), as shown in Fig. 9. The parameters are: $U_g = 220$ V, $U = 210$ V, $\omega_N = 50\times2\times3.14$ rad/s, $L = 5$ mH, $X = \omega_N L$, $J = 0.02$ kg·m^2; $D = 0.1$. From the magnitude and phase curves, it can be seen that the cut-off frequency of the active power transfer function controlled by the VSG control is relatively small, which means the power response speed is slow. As can be seen from (16), the power fluctuation of the second order harmonic will appear in the output power. In the VSG control, the average power is applied in the power calculation process, which is equivalent to filtering out the disturbance of the second order harmonic power fluctuation. Therefore, the disturbance of the second order harmonic power fluctuation has a small influence on the original power control based on the average power control, and the main influence is still on the DC side fluctuation.

$$G_1(s) = \frac{P(s)}{P_{\text{ref}}(s)} = \frac{\frac{U_g U}{J\omega_N X}}{s^2 + \frac{D}{J}s + \frac{U_g U}{J\omega_N X}} \tag{14}$$

$$\begin{cases} \omega_n = \sqrt{\frac{U_g U}{J\omega_N X}} \\ \xi = \frac{D}{2}\sqrt{\frac{\omega_N X}{J U_g U}} \end{cases} \tag{15}$$

$$G_2(s) = \frac{\Delta P(s)}{P(s)} = \frac{s^2 + \frac{D}{J}s}{s^2 + \frac{D}{J}s + \frac{U_g U}{J\omega_N X}}. \tag{16}$$

3. Simulation Results

To verify the effectiveness of the proposed method, the simulation is presented in this part. The simulation model is built. The main circuit and the control circuit are proposed. Under the situation of unbalanced grid voltage, the simulation of the strategy proposed in this paper is presented in Fig. 10, in which the simulation software PSIM is used. In Fig. 10(a), the main circuit includes the inverter and the grid. The control system includes the droop control, the VSG control, and the voltage current dual control loop. The control system is shown in Fig. 10(b). The droop control, the VSG control, the voltage current dual control loops, and the proposed control strategy for suppressing the fluctuation are presented.

The simulation waveforms are shown in this part. The verification of the proposed control method is achieved. And, the comparison of the dynamic response is also proposed. The simulation waveform is shown in Fig. 11. In Fig. 11(a), the voltage simulation waveform under a three-phase unbalanced grid is shown. The voltages of phases a, b, and c are unbalanced. In Fig. 11(b), in the traditional control method, the dynamic performance of the negative current control may influence the dynamic process of the suppression method. In Fig. 11(c), due to the unbalanced grid voltage, a power fluctuation at twice the fundamental frequency is generated, and the dynamic process is short than the tradition method. The traditional strategy is a closed-loop control, while the proposed strategy employs open-loop control. In term of the dynamic response, the proposed suppression strategy has a faster dynamic

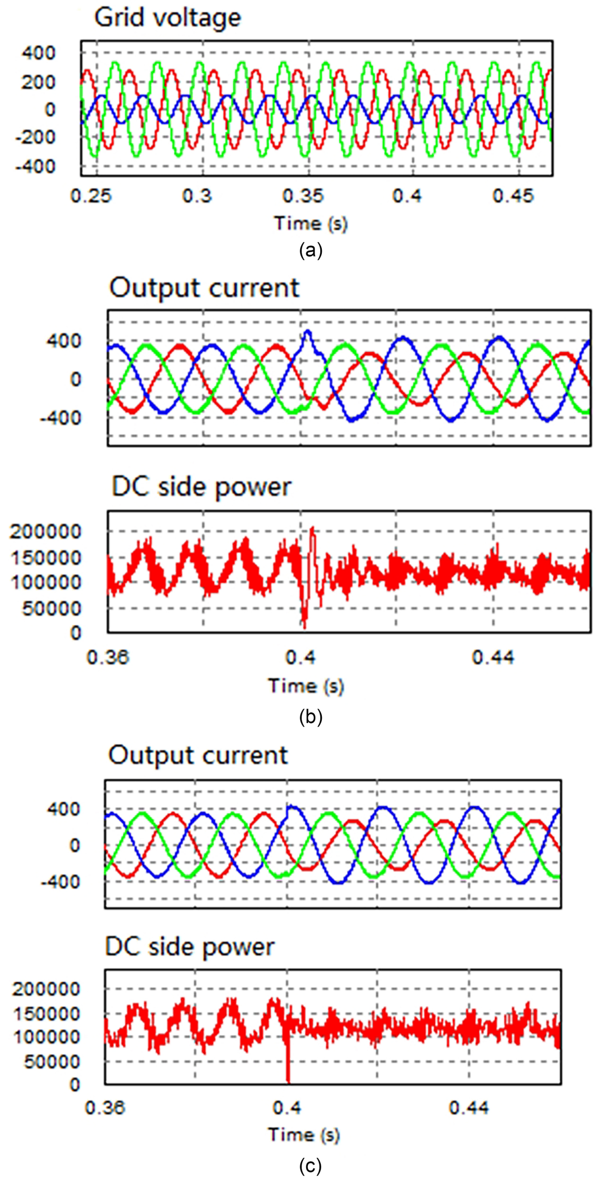

Figure 11. Simulation results of proposed suppression strategy: (a) grid voltage; (b) output current and DC side power (traditional control method); and (c) output current and DC side power (proposed control method).

response than that of the traditional suppression strategy. Under these conditions, the output current of the inverter with the VSG control is the balanced three-phase current. When the power fluctuation suppression strategy proposed in this paper is applied as shown in Fig. 10(b), the output current of the inverter with the VSG control becomes the unbalanced three-phase current, and there is not a power fluctuation at twice the fundamental frequency. The simulation results verify the effectiveness of the suppression strategy proposed in this paper.

4. Experimental Results

The experiment results are provided. The experimental waveforms are shown in this part. The conclusion is verified. The experimental platform and the experimental results

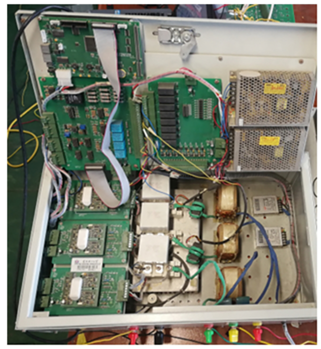

(a)

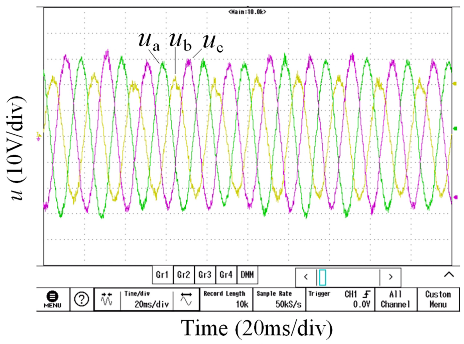

(a)

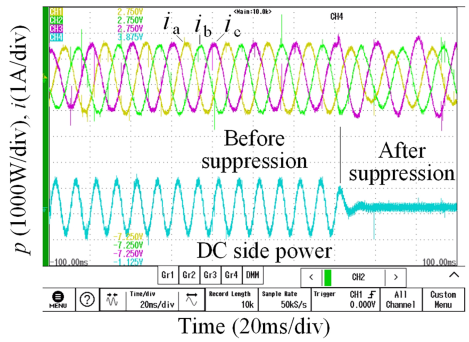

(b)

Figure 12. Experiment results of proposed suppression strategy: (a) experimental platform; (b) grid voltage; and (c) experimental waveforms of AC current and DC side power before and after suppression.

are shown in Fig. 12, where the waveform of the three-phase unbalanced voltage is presented in Fig. 12(b). The experimental platform includes a main circuit shown in Fig. 3. And, the control system includes the driving circuit, the controller and the measure circuit. The controller is based on the DSP28335. The power of the experimental platform is about 10 kW, and the VSG control strategy is used. The control strategy is realised in the DSP28335, including the droop control, the voltage current dual control loop, the VSG control, and the proposed control strategy. The parameters of the experimental platform are: U_{dc} = 200 V, U = 70 V, ω_N = 50×2×3.14 rad/s, L = 0.5 mH, L_g = 3 mH, C = 50 μF. In Fig. 12(c), due to the unbalanced voltage of the power grid, a power fluctuation at twice the fundamental frequency is generated on the DC side of the inverter. The output current of the inverter with the VSG control is a balanced three-phase current. When the power fluctuation suppression control strategy proposed in this paper is applied, the output current of the inverter with the VSG control becomes the unbalanced three-phase current, and the power obtained by the interaction with the unbalanced three-phase voltage does not includes the power fluctuation at twice the fundamental frequency, which proves the effectiveness of the power fluctuation suppression strategy proposed in this paper.

5. Conclusions

In order to solve the problem of power fluctuation on the DC side of inverters with VSG control under unbalanced grid voltage, this paper proposes a direct-feedforward-voltage control strategy to suppress DC side power fluctuations in inverters. The conclusions are as follows: The inverter with VSG control can output an additional voltage, which interacts with the positive sequence current and the unbalanced grid voltage to eliminate the DC side power fluctuations at twice the fundamental frequency; The feedforward voltage is obtained from the positive and negative sequence voltages, positive and negative sequence currents, and positive and negative sequence output voltages of the power grid; the proposed strategy responds quickly and has a better suppression effect on the power fluctuation in the dynamic process; the simulation and experimental results verify the effectiveness of the power fluctuation suppression strategy proposed in this paper.

References

[1] Z. Li, J. Zhang, H. Wang, and Y.J. Bao, Fatigue performance of power transmission tower system based on wind vibration fatigue, *International Journal of Power and Energy Systems,* , *44*(10), 2024, 1–8.

[2] Y. Sun, Z. Zhao, M. Yang, D. Jia, W. Pei, and B. Xu, Overview of energy storage in renewable energy power fluctuation mitigation, *CSEE Journal of Power and Energy Systems*, *6*(1), 2020, 160–173.

[3] W. Mao, S. Yang, and X. Gao, Modelling and optimisation of green energy system based on complementary integration of renewable energy, *International Journal of Power and Energy Systems, 44*(10), 2024, 1–8.

[4] S.H. Abdallah and S. Tounsi, Optimal design and control of AC-DC-DC wind energy system for electric vehicle batteries recharging stations, *International Journal of Power and Energy Systems, 44*(10), 2024, 1–8.

[5] S. Dong and Y.C. Chen, Adjusting synchronverter dynamic response speed via damping correction loop, *IEEE Transactions on Energy Conversion*, *32*(2), 2017, 608–619.

[6] K. S. Ratnam, K. Palanisamy, and G. Yang, Future low-inertia power systems: requirements, issues, and solutions - a review, *Renewable and Sustainable Energy Reviews*, *124*, 2020, 1–24.

[7] X. Liang, C. Andalib-Bin-Karim, W. Li, M. Mitolo, and M.N.S.K. Shabbir Adaptive virtual impedance-based reactive power sharing in virtual synchronous generator controlled microgrids, *IEEE Transaction on Industry Application*, , *51*(7), 2021, 463–60.

[8] K. Koiwa, K. Inoo, T. Zanma, and K.-Z. Liu, Virtual voltage control of VSG for overcurrent suppression under symmetrical and asymmetrical voltage dips, *IEEE Transactions on Industrial Electronics*, *69*(11), 2022, 11177–11186.

[9] H. Wang, X. Zhang, H. Yan, H. Jia, and Y. Li, Design of control parameters and multi-objective control strategy of virtual synchronous generator under unbalanced voltage, in *Proceeding of the 4th International Conference on Advanced Electrical and Energy Systems (AEES)*, Shanghai, 2023, 258–263.

[10] Z. Wang, Y. Yu, W. Gao, M. Davari, and C. Deng, Adaptive, optimal, virtual synchronous generator control of three-phase grid-connected inverters under different grid conditions—An adaptive dynamic programming approach, *IEEE Transactions on Industrial Informatics*, *18*(11), 2022, 7388–7399.

[11] F. Li, G. Liu, K. Zhu, and W. Wang, An improved control strategy of virtual synchronous generator under unbalanced conditions, in *Proceeding of the IEEE 4th Southern Power Electronics Conference (SPEC)*, Singapore, 2018, 1–6.

[12] W. Xu, W. Zhu, and Z. Shu, Suppression of DC voltage ripple impact on non-isolated single-phase half-bridge unified power quality conditioner, *IEEE Transactions on Industrial Electronics*, *71*(9), 2024, 10523–10532.

[13] S. Yazdani, M. Ferdowsi, M. Davari, and P. Shamsi, Advanced current-limiting and power-sharing control in a PV-based grid-forming inverter under unbalanced grid conditions, *IEEE Journal of Emerging and Selected Topics in Power Electronics*, *8*(2), 2020, 1084–1095.

[14] C. Liu, D. Xu, N. Zhu, F. Blaabjerg, and M. Chen, DC-voltage fluctuation elimination through a dc-capacitor current control for DFIG converters under unbalanced grid voltage conditions, *IEEE Transactions on Power Electronics*, 28(7), 2013, 3206–3218.

[15] Y. Song and H. Nian, Modularized control strategy and performance analysis of DFIG system under unbalanced and harmonic grid voltage, *IEEE Transactions on Power Electronics*, *30*(9), 2015, 4831–4842.

[16] M.M. Baggu, B.H. Chowdhury, and J.W. Kimball, Comparison of advanced control techniques for grid side converter of doubly-fed induction generator back-to-back converters to improve power quality performance during unbalanced voltage dips, *IEEE Journal of Emerging and Selected Topics in Power Electronics*, 3(2), 2015, 516–524.

[17] T. Yin, Y. Wang, J. Sun, X. Li, B. Yue, X. Wang, P. Liu, Y. Peng, Y. Liu, and P. Li, Impedance-based characterization of positive–negative sequence separation and its effects on MMC-HVDC stability, *IEEE Journal of Emerging and Selected Topics in Power Electronics*, *10*(4), 2022, 4395–4411.

[18] M.M. Haque, M.S. Ali, P. Wolfs, and F. Blaabjerg, A UPFC for voltage regulation in LV distribution feeders with a DC-link ripple voltage suppression technique, *IEEE Transactions on Industry Applications*, , *56*(6), 2020, 6857–6870.

[19] J. Li, S.-Y. Chen, and X.-L. Li, Power Oscillation suppression strategy for virtual synchronous generators under unbalanced grid conditions based on novel power reference calculation method, in *Proceeding of the IEEE 9th International Power Electronics and Motion Control Conference (IPEMC2020-ECCE Asia)*, Nanjing, 2020, 2906–2911.

[20] T. Zheng, L. Chen, H. Zhang, T. Chen, and S. Mei, Control strategy for suppressing power oscillation of virtual synchronous generator under unbalanced grid voltage, in *Proceeding of the International Conference on Renewable Power Generation (RPG)*, , Beijing, 2015, 1–5.

[21] D. Liang, C. Qin, J. Zong, X. Wu, J. Mei, and B. Wang, Unbalanced control strategy of improved virtual synchronous generator in power grid, in *Proceeding of the IEEE 8th Annual International Conference on CYBER Technology in Automation, Control, and Intelligent Systems (CYBER)*, 2018, Tianjin, 1311–1316.

[22] L. Chen, J. Tang, X. Qiao, H. Chen, and Z. Zhao, Study of resistive SFCLs for transient stability enhancement of paralleled synchronous and virtual synchronous generators in weak grid, *IEEE Transactions on Industry Applications*, *59*(3), 2023, 3044–3055.

[23] L. Chen, X. You, Z. Li, H. He, M. Yang, S. Zheng, J. Tang, and H. Chen, Optimal impedance reshaping approach for inhibiting subsynchronous oscillation in virtual synchronous generator based on SMES-battery, *IEEE Transactions on Applied Superconductivity*, *34*, (8), 2024, 3801406.

[24] I. Khan, A.S. Vijay, and S. Doolla, Evaluating power sharing performance of distributed generators in microgrids with hybrid sources and mixed tie-lines, *IEEE Transactions on Industry Applications*, , *59*(5), 2023, 5363–5375.

[25] A. Moulichon, M. Alamir, V. Debusschere, L. Garbuio, M.A. Rahmani, M.-X. Wang, and N. Hadjsaid, Observer-based current controller for virtual synchronous generator in presence of unknown and unpredictable loads, *IEEE Transactions on Power Electronics*, *36*(2), 2021, 1708–1716.

[26] D. Terazono, J. Liu, Y. Miura, S. Sakabe, H. Bevrani, and T. Ise, Grid frequency regulation support from back-to-back motor drive system with virtual-synchronous-generator-based coordinated control, *IEEE Transactions on Power Electronics*, *36*(3), 2021, 2901–2913.

[27] J. Zhou, H. Sun, Y. Xu, R. Han, Z. Yi, L. Wang, and J.M. Guerrero, Distributed power sharing control for islanded single-/three-phase microgrids with admissible voltage and energy storage constraints, *IEEE Transactions on Smart Grid*,*12*(4), 2021, 2760–2775.

[28] K. Sun, W. Yao, J. Wen, and L. Jiang, A two-stage simultaneous control scheme for the transient angle stability of VSG considering current limitation and voltage support, *IEEE Transactions on Power System*, *37*(3), 2022, 2137–2150.

Biographies

Wangwang Bai received the B.S. and M.S. degrees from Northeast Electric Power University, China, in 2013 and 2017, respectively. He has been a Senior Engineer with the State Grid Gansu Electric Power Company in 2025. His research interests include grid planning and source-grid coordination analysis.

Dezhou Yang received the B.S. and M.S. degrees from North China Electric Power University, China, in 1992 and 1996, respectively. He has been a Senior Engineer with the State Grid Gansu Electric Power Company in 2021. His research interests include grid planning and source-grid coordination analysis.

Zhongdan Zhang received the B.S. degree from North China Electric Power University, China, in 2003, and the M.S. degree from Xi'an Jiaotong University in 2015. He has been a Senior Engineer with the State Grid Gansu Electric Power Company in 2014. His research interests include transmission network planning technology.

Wanwei Li received the B.S. degree from Tianjin University, China, in 2005, and the M.S. degree from Xi'an Jiaotong University, in 2011. He has been a Senior Engineer with the State Grid Gansu Electric Power Company in 2014. His research interests include power dispatch operation control.

Ping Cai received the B.S. and M.S. degrees from Wuhan University, China, in 2018 and in 2021, respectively. She has been an Intermediate Engineer with the State Grid Gansu Electric Power Company in 2021. Her research interests include transmission network planning technology.